On Structural and Safety Properties of Head-to-Tail String Stability in Mixed Platoons

Liu, Di; Besselink, Bart; Baldi, Simone; Yu, Wenwu; Trentelman, Harry L.

Published in:
IEEE Transactions on Intelligent Transportation Systems

DOI:
10.1109/TITS.2022.3151929

Publication date:
2023

On Structural and Safety Properties of Head-to-Tail String Stability in Mixed Platoons

Di Liu, *Member, IEEE*, Bart Besselink, *Member, IEEE*, Simone Baldi, *Senior Member, IEEE*, Wenwu Yu, *Senior Member, IEEE*, and Harry L. Trentelman, *Life Fellow, IEEE*

***Abstract*— The interaction between automated and human-driven vehicles in mixed (human/automated) platoons is far from understood. To study this interaction, the notion of head-to-tail string stability was proposed in the literature. Head-to-tail string stability is an extension of the standard string stability concept where, instead of asking every vehicle to achieve string stability, a lack of string stability is allowed due to human drivers, provided it can be suitably compensated by automated vehicles sparsely inserted in the platoon. This work introduces a theoretical framework for the problem of head-to-tail string stability of mixed platoons: it discusses a suitable vehicle-following human driver model to study mixed platoons, and it gives a reduced-order design strategy for head-to-tail string stability only depending on three gains. The work further discusses the safety limitations of the head-to-tail string stability notion, and it shows that safety improvements can be attained by an appropriate reduced-order design strategy only depending on two additional gains. To validate the effectiveness of the design, linear and nonlinear simulations show that the string stability/safety trade-offs of the proposed reduced-order design are comparable with those resulting from full-order designs.**

***Index Terms*— Mixed platoons, automated vehicles, string stability, head-to-tail string stability, human driving model.**

I. Introduction

In RECENT years, the topic of automated vehicles has been investigated from different perspectives, ranging from computer vision and communication to control. With respect to control, it is of interest to investigate if and how *platoons of automated vehicles* can improve the traffic flow: a pioneering result in this direction was by Peppard [1], which introduced the problem of 'string stability', i.e. the capability of a platoon of automated vehicles to reject disturbances in the traffic flow. Characterizations of string stability have been later given in the Lyapunov stability framework [2] and in the frequency domain [3]. These characterizations have been improved in different directions, such as having the platoon moving on the plane [4], letting the vehicles communicate with both preceding and following vehicles [5], [6], communicate through various patterns [7], [8] or with constraints [9], [10] (cf. the survey on string stability [11]). Recent results include a delay-based spacing policy [12], modeling automated vehicles by partial differential equations [13], and dealing with heterogeneity in vehicle dynamics [14]–[18]. Limitations or impossibility of string stability in the absence of communication was studied both theoretically [19], [20] and experimentally [21].

In parallel with the study of platoons of automated vehicles, research has been devoted to *platoons of human-driven vehicles*, with the aim to understand how human drivers follow each other and how phenomena such as stop-and-go waves originate from human vehicle-following behavior. In this respect, two classical models of human vehicle-following behavior are the optimal velocity model [22] and the intelligent driver model [23]. Extensions to these models have appeared in various directions [24]–[26]. Real-life experiments with human drivers running on a cyclic path [27] have also stimulated interest in studying cyclic interconnections [28].

Before allowing automated vehicles in real traffic, it is important to study how these vehicles interact with human-driven vehicles. From this observation, an increasing interest in *mixed (human/automated) traffic* has arisen: [29] studied how the traffic fundamental diagram (flow vs. density) changes in the presence of mixed traffic; [30], [31] studied how to calibrate vehicle-following models in mixed traffic; real experiments with human-driven and automated vehicles driving on a cyclic path have been performed [32]; studies on stability of mixed traffic were reported [33]–[35]; new definitions of string stability for mixed traffic appeared [36], [37]; optimal control [38], [39] and mitigation of oscillations [40], [41] in mixed traffic were studied. Note that most of these studies, including our study: rely on linear systems theory using linearization of the human vehicle-following model; consider the optimal velocity model [22] as human vehicle-following model due to its simpler formulation; consider the technologically feasible scenario in which the human-driven vehicles, while being uncontrolled (i.e. acting autonomously according the vehicle-following model), can communicate their position/velocity/acceleration to allow the

Manuscript received 23 June 2021; revised 17 November 2021 and 2 February 2022; accepted 9 February 2022. Date of publication 23 February 2022; date of current version 31 May 2023. This work was supported in part by the National Natural Science Foundation of China under Grant 62073074, Grant 61673107, and Grant 62073076; in part by the Double Innovation Plan under Grant 4207012004; in part by the Special Funding for Overseas under Grant 6207011901; in part by the Research Fund for International Scientists under Grant 62150610499; and in part by the Jiangsu Provincial Key Laboratory of Networked Collective Intelligence under Grant BM201700. The Associate Editor for this article was Z. Zheng. *(Corresponding authors: Wenwu Yu; Simone Baldi.)*

Di Liu is with the School of Cyber Science and Engineering, Southeast University, Nanjing 211189, China, and also with the Bernoulli Institute for Mathematics, Computer Science and Artificial Intelligence, University of Groningen, 9712 CP Groningen, The Netherlands (e-mail: di.liu@rug.nl).

Bart Besselink and Harry L. Trentelman are with the Bernoulli Institute for Mathematics, Computer Science and Artificial Intelligence, University of Groningen, 9712 CP Groningen, The Netherlands (e-mail: b.besselink@rug.nl; h.l.trentelman@rug.nl).

Simone Baldi and Wenwu Yu are with the Frontiers Science Center for Mobile Information Communication and Security, School of Mathematics, Southeast University, Nanjing 211189, China, and also with the Purple Mountain Laboratories, Nanjing 211100, China (e-mail: s.baldi@tudelft.nl; wwyu@seu.edu.cn).

Digital Object Identifier 10.1109/TITS.2022.3151929

automated vehicle to make decisions based on the surrounding traffic.

Due to the autonomous (i.e. uncontrolled) behavior of human-driven vehicles, it is clear that mixed traffic requires different stability and string stability methodologies compared to automated traffic [42]. The notion of *head-to-tail string stability* was originally proposed in [43] and further studied in [36], [44], [45]. Instead of making every vehicle address string stability, head-to-tail string stability allows a lack of string stability due to human drivers, provided it can be suitably compensated by one or more automated vehicles sparsely inserted in the traffic flow. The literature has shown that when human-driven and automated vehicles only interact with the preceding vehicle, head-to-tail string stability can be attained by increasing the number of automated vehicles in the platoon [44], [45]; alternatively, it was proposed in [36] that the automated vehicle uses information from multiple preceding human-driven vehicles for feedback control. The multi-communication scenario is used in several other studies on mixed traffic [32], [35], [38], [39], including this study.

Several works have shown that head-to-tail string stability of mixed platoons can be formulated as appropriate $\mathcal{H}_\infty$ control problems [36], [44], [45]. Even though such problems can be solved numerically, an analytic treatment of head-to-tail string stability of mixed platoons is still missing. In this work, we introduce a theoretical framework for the problem of head-to-tail string stability of mixed platoons. The framework we propose departs from earlier ones in the following aspects:

a) from a vehicle dynamics point of view, the framework starts from a vehicle-following model that we propose as a synthesis of the models used in the automated vehicle literature and the human-driven vehicle literature;
b) from an analytic point of view, a new reduced-order head-to-tail string stability design is proposed that essentially *depends on only three control gains* (cf. the structural properties of head-to-tail string stability in Theorem 2 and the reduced-order design of Theorem 3). This marks a difference with the aforementioned $\mathcal{H}_\infty$ designs since the complexity of the proposed control design does not depend on the length of the platoon;
c) we show that control design for head-to-tail string stability generally does not lead to safe designs, where safety is understood as the ability to maintain the desired inter-vehicle distance. Based on this, we propose an extended controller that is aimed at improving safety while remaining of reduced order (cf. the structural properties of safety in Remark 4 and the reduced-order design of Theorem 4).

Simulations with linear and nonlinear vehicle models show that the proposed reduced-order design has similar characteristics as those obtained from large-scale $\mathcal{H}_\infty$ control problems.

The rest of the paper is organized as follows. In Section II, we propose a human vehicle-following model to study mixed platoons. In Section III, we study platoons of human-driven vehicles and conclude that human-behavior parameters proposed in the literature result in a stable but not string stable platoon. Section IV presents a new reduced-order strategy for the string stability of mixed platoons. Section V analyzes a reduced-order method for safety improvement. Simulations in Section VI are followed by conclusions in Section VII.

Notation The sets of real numbers and real $n \times m$ matrices are denoted by $\mathbb{R}$ and $\mathbb{R}^{n\times m}$, respectively. The $q \times q$ identity matrix is denoted by I_q. For any $W \in \mathbb{R}^{n\times m}$ with rank m, the annihilator $W^\perp \in \mathbb{R}^{(n-m)\times n}$ of W is any full row rank matrix such that $W^\perp W = 0$.

II. Vehicle-Following Model Description

In this section we recall a standard model for vehicle-following human behavior and we propose our own vehicle-following model, used to study mixed traffic scenarios.

A. Background on Optimal Velocity Model

The *optimal velocity model (OVM)* was originally proposed in [22] as a model for vehicle-following human behavior. The model assumes that during the vehicle-following task, human drivers aim at a desired velocity,[1] which depends on the relative distance to the preceding vehicle. By denoting the preceding vehicle with index $i+1$, the optimal velocity behavior of vehicle i is described as

$$\begin{aligned} \dot{s}_i(t) &= v_i(t), \\ \dot{v}_i(t) &= \alpha\left[V\left(d_i\left(t\right)\right) - v_i\left(t\right)\right] + \beta\left[v_{i+1}\left(t\right) - v_i\left(t\right)\right], \end{aligned} \quad (1)$$

where s_i and v_i denote position and velocity of vehicle i, $d_i = s_{i+1} - s_i$ indicates the distance between the two vehicles, α and β are positive constants that represent human-driving feedback, and $V(d)$ is a nonlinear sigmoidal function that characterizes the desired velocity, such as

$$V(d) = \begin{cases} 0 & \text{if } d \le d_l \\ \dfrac{v_{\max}}{2}\left[1 - \cos\left(\pi \dfrac{d - d_l}{d_u - d_l}\right)\right] & \text{if } d_l < d \le d_u \\ v_{\max} & \text{if } d > d_u \end{cases} \quad (2)$$

The meaning of (2) is: when the spacing is smaller than the lower bound d_l, the desired velocity equals 0; when the spacing is larger than the upper bound d_u, the desired velocity equals a maximum velocity $v_{\max}$; in between these values, the desired velocity is a monotonically-increasing function of d.

When linearized around an equilibrium d^* and $v^* = V(d^*)$, the optimal velocity model (1)-(2) takes the form

$$\begin{aligned} \dot{s}_i(t) &= v_i(t), \\ \dot{v}_i(t) &= \alpha\kappa\left[s_{i+1}(t) - s_i(t) - \frac{v_i(t)}{\kappa}\right] + \beta\left[v_{i+1}(t) - v_i(t)\right], \end{aligned}$$

where $\kappa := V'(d^*)$. For compactness, the linearized OV model is sometimes written as

$$\begin{aligned} \dot{s}_i(t) &= v_i(t), \\ \dot{v}_i(t) &= be_i(t) + cv_i(t), \end{aligned} \quad (3)$$

where $e_i = s_{i+1} - s_i - hv_i$ is the velocity-dependent spacing error (hereafter simply referred to as spacing error), $v_i = v_{i+1} - v_i$ is the relative velocity, and we denote $b = \alpha\kappa$, $c = \beta$, $h = \frac{1}{\kappa}$. Note the two feedback actions of human behavior in (3): a proportional action depending on the spacing error, and a derivative action depending on the relative velocity.

[1]The term 'optimal' was used historically to indicate such a desired velocity and it does not refer to an optimal control problem.

B. Proposed Human-Driven Model

A form of velocity-dependent spacing error e_i similar to the one in (3) appears in the automated vehicle literature (e.g. [3], [14]). There, a velocity-dependent desired spacing is taken as

$$d_{r,i}(t) = hv_i(t),$$

so that the spacing error also becomes $e_i(t) = d_i(t) - d_{r,i}(t) = s_{i+1}(t) - s_i(t) - hv_i(t)$. In the automated vehicle literature, $h > 0$ is referred to as *time headway*, because it quantifies the inter-vehicle time gap. The analogy between the time-headway spacing and the OVM velocity-dependent spacing error in (3) provides a motivation for exploring this analogy in the OVM framework. To this purpose, we note that the vehicle dynamics of automated vehicles is often represented as

$$\tau \dot{a}_i(t) = -a_i(t) + u_i(t), \tag{4}$$

where u_i is the input (desired acceleration) to the vehicle, and $\tau > 0$ is the engine time constant representing the time necessary to reach a desired acceleration due to the engine dynamics [3], [14]. Modelling the engine dynamics with a time constant τ was originally proposed in [46] and adopted in virtually all automated vehicle literature with engine dynamics. Motivated by the fact that also human-driven vehicles unavoidably have an engine, it is natural to think of the human-driving feedback in (3) as an input u_i provided by the human driver to the engine. As a result, we propose the following model for (linear) vehicle-following human behavior

$$\begin{aligned} \dot{s}_i(t) &= v_i(t), \\ \dot{v}_i(t) &= a_i(t), \\ \tau \dot{a}_i(t) &= -a_i(t) + be_i(t) + cv_i(t). \end{aligned} \tag{5}$$

The main difference between (3) and (5) is that the latter takes into account the time neeeded to reach a desired acceleration due to the engine dynamics. This time constant is either unmodelled in the vehicle-following literature, or modelled as an adaptation time needed to accelerate to a new desired velocity [26]. This is because driver behavioral models traditionally have no control design purpose, and focus on the actual rather than the desired acceleration. In this sense, the proposed model (5) has the merit of unifying in a control sense models of human drivers and models appearing in the automated vehicle literature. From a control perspective, the time constant τ can also be regarded as a first-order approximation [47, Chap. 6] of the reaction time typical of human-driving behavior. In the following sections, we will see how models with a structure as (5) can be used to study mixed traffic scenarios with both human-driven and automated vehicles.

III. Platoons of Human-Driven Vehicles

A preliminary step in studying mixed traffic scenarios is to study the properties of platoons of human-driven vehicles. When the focus is on mathematical analysis, a standard assumption in the literature is to assume homogeneous characteristics for all vehicles (cf. [29], [30], [32]–[35] among others). This amounts to assuming that all human-driven vehicles have the same constants τ, b, c, and h.

Consider a platoon with N human-driven vehicles indexed in such a way that vehicle 1 is the last vehicle of the platoon: the reason why we have chosen this 'forward' notation (the leading vehicle has the largest index) will become clear in Section IV where an automated vehicle will be placed at the end of the platoon and indexed as vehicle 0. In order to study stability, assume that a vehicle $N+1$ moves autonomously in front of the platoon with dynamics given by

$$\begin{aligned} \dot{v}_{N+1} &= a_{N+1}, \\ \tau \dot{a}_{N+1} &= -a_{N+1} + u_{N+1}. \end{aligned} \tag{6}$$

If $u_{N+1} = 0$, then in steady state vehicle $N+1$ has constant velocity. In general, u_{N+1} acts as an external disturbance to vehicle $N+1$, which can be used to study disturbance propagation. For vehicles $i = N, \ldots, 1$, we consider the state variables e_i, v_i, a_i with the following dynamics

$$\begin{aligned} \dot{e}_i(t) &= v_i(t) - ha_i(t), \\ \dot{v}_i(t) &= a_{i+1}(t) - a_i(t), \\ \tau \dot{a}_i(t) &= -a_i(t) + be_i(t) + cv_i(t). \end{aligned} \tag{7}$$

As a first step, we analyze *stability of a platoon of human-driven vehicles*. We call the platoon stable if we have $(e_i(t), v_i(t), a_i(t)) \to 0$ as $t \to \infty$ for all initial states $(e_i(0), v_i(0), a_i(0)), i = N, \cdots, 1$ and all initial conditions $(v_{N+1}(0), a_{N+1}(0))$ of the leading vehicle $N+1$ with $u_{N+1} = 0$. The following result holds.

Theorem 1 (Stability of Platoons of Human-Driven Vehicles):The platoon of N human-driven vehicles with dynamics as in (7) *is stable if and only if the following conditions hold*

$$\tau > 0, \quad b > 0, \quad bh + c > b\tau. \tag{8}$$

Proof: In compact form, (7) can be written as

$$\dot{x}_i = A_0 x_i + E_0 C_0 x_{i+1}, \quad i = N, \ldots, 1,$$

with $x_i := \begin{bmatrix} e_i & v_i & a_i \end{bmatrix}^T$,

$$A_0 := \begin{bmatrix} 0 & 1 & -h \\ 0 & 0 & -1 \\ \frac{b}{\tau} & \frac{c}{\tau} & -\frac{1}{\tau} \end{bmatrix}, E_0 := \begin{bmatrix} 0 \\ 1 \\ 0 \end{bmatrix}, C_0 := \begin{bmatrix} 0 & 0 & 1 \end{bmatrix}. \tag{9}$$

Thus, the dynamics of the platoon of N human-driven vehicles is represented by

$$\begin{bmatrix} \dot{x}_N \\ \dot{x}_{N-1} \\ \vdots \\ \dot{x}_1 \end{bmatrix} = \begin{bmatrix} A_0 & 0 & \cdots & 0 & 0 \\ E_0C_0 & A_0 & \cdots & 0 & 0 \\ \vdots & \ddots & \ddots & \vdots & \vdots \\ 0 & 0 & \cdots & E_0C_0 & A_0 \end{bmatrix} \begin{bmatrix} x_N \\ x_{N-1} \\ \vdots \\ x_1 \end{bmatrix} + \begin{bmatrix} E_0 \\ 0 \\ \vdots \\ 0 \end{bmatrix} a_{N+1}. \tag{10}$$

Note that the leading vehicle (6) is only implicitly included in (10) through its acceleration a_{N+1}, which is regarded as an input to the platoon of human-driven vehicles. Due to the block-lower-triangular structure of the state matrix in (10) and the fact that the evolution of a_{N+1} is a solution to the stable linear systems (6) with $u_{N+1} = 0$, the platoon is stable if and only if A_0 is Hurwitz; A_0 has characteristic polynomial

$\tau\lambda^3 + \lambda^2 + (bh + c)\lambda + b$. According to the Routh-Hurwitz criterion, A_0 is Hurwitz if and only if the conditions (8) hold. □

Remark 1 (Stability of Human Parameters in the Literature): In the literature on human-driven vehicles, specific numerical values for b, c, h (e.g. identified from real-life tests [48], [49]) are taken. The following three representative sets of parameters can be found in [35]–[37], respectively:

1) $b = 0.12, c = 0.4, h = 5/3$ (linearized at $v^* = 29$ m/s),
2) $b = 0.9, c = 0.9, h = 2/3$ (linearized at $v^* = 15$ m/s),
3) $b = 0.6, c = 0.15, h = 5/6$ (linearized at $v^* = 9$ m/s).

It can be verified that all three sets of parameters satisfy the stability conditions (8) as long as $\tau < 1$. Therefore, since the literature on automated vehicles indicates that engine dynamics is in the range $\tau \in [0.1, 0.3]$, we conclude that all human-driven parameters above result in a stable platoon.

IV. String Stability of Mixed Platoons

In addition to stability, the notion of string stability is a crucial in platooning [1]–[3]. String stability refers to the capability to attenuate exogenous inputs (e.g. leader input) as they propagate through the platoon. To formalize this, we rewrite the state space representation (7) of vehicle i as

$$\begin{aligned} \dot{x}_i &= A_0 x_i + E_0 a_{i+1}, \\ a_i &= C_0 x_i. \end{aligned} \tag{11}$$

Thus, the transfer function from a_{i+1} to a_i is given by

$$G(s) := C_0(sI - A_0)^{-1}E_0 = \frac{cs + b}{\tau s^3 + s^2 + (bh + c)s + b}. \tag{12}$$

The rationale behind (11) (or (12)) is to consider the acceleration of the preceding vehicle $i + 1$ as a disturbance to vehicle i. Because the denominator of (12) is the characteristic polynomial of A_0, $G(s)$ is stable if the stability conditions of Theorem 1 are satisfied. As a result, the $\mathcal{H}_\infty$ norm of the transfer function $G(s)$ can be used as a measure of amplification from a_{i+1} to a_i. With this motivation, we recall the following definition of string stability based on the $\mathcal{H}_\infty$ norm, or equivalently the induced $\mathcal{L}_2$-gain [3].

Definition 1 ($\mathcal{L}_2$ String Stability): Consider a platoon of homogeneous vehicles interacting along a string according to (11)*. Let $G(s)$ be the transfer function from a_{i+1} to a_i. If*

$$\|G(s)\|_\infty \leq 1,$$

then the platoon is called string stable.

Unfortunately, differently from automated vehicles, human-driven vehicles do not[2] satisfy $\|G(s)\|_\infty \leq 1$, neither have control inputs to attain string stability via appropriate design of b and c [50]–[52]. Therefore, string stability in mixed traffic cannot be approached in the same way as Definition 1. This will be formalized in the following subsection.

A. Head-to-Tail String Stability Scenario

The fact that human-driven vehicles do not exhibit string stable behavior motivates the idea of sparsely placing automated vehicles in the traffic, with the aim to achieve (some notion of) string stability. Consider a mixed platoon scenario as sketched in Fig. 1: the mixed platoon is composed of the previously introduced N human-driven vehicles, followed by one automated vehicle indexed with 0 and with dynamics

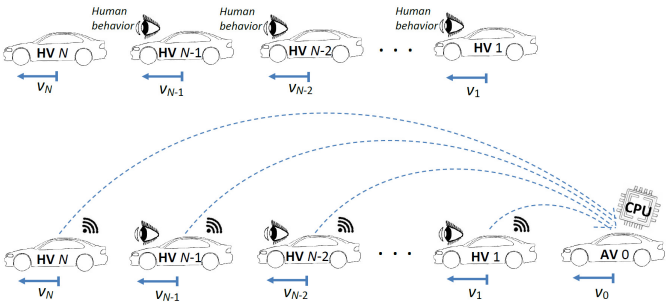

Fig. 1. Notation used for platoons of human vehicles and for mixed platoons.

$$\begin{aligned} \dot{x}_0 &= A_1 x_0 + B_0 u + E_0 a_1, \\ x_0 &:= \begin{bmatrix} e_0 \\ v_0 \\ a_0 \end{bmatrix}, \quad A_1 := \begin{bmatrix} 0 & 1 & -h \\ 0 & 0 & -1 \\ 0 & 0 & -\frac{1}{\tau} \end{bmatrix}, \quad B_0 := \begin{bmatrix} 0 \\ 0 \\ \frac{1}{\tau} \end{bmatrix}, \end{aligned} \tag{13}$$

and E_0 the same as in (9). The subscript 1 in A_1 refers to vehicle 1 preceding the automated vehicle 0. A practical reason for adopting a notation in which the automated vehicle the smallest index is that one may want the automated vehicle to keep index 0 even when N changes. This may represent the fact that new human vehicles lead or merge in the platoon. With this in mind, we refer to the control input u_0 of the automated vehicle simply as u (to be designed), as reported in (13). The overall mixed platoon model is given by

$$\begin{aligned} \dot{x} &= Ax + Bu + Ea_{N+1}, \\ a_0 &= Cx. \end{aligned} \tag{14}$$

where

$$x := \begin{bmatrix} x_N \\ x_{N-1} \\ \vdots \\ x_0 \end{bmatrix}, \quad A := \begin{bmatrix} A_0 & 0 & 0 & \cdots & 0 \\ E_0C_0 & A_0 & 0 & \cdots & 0 \\ 0 & E_0C_0 & A_0 & \vdots & \vdots \\ \vdots & \vdots & \ddots & A_0 & 0 \\ 0 & 0 & \cdots & E_0C_0 & A_1 \end{bmatrix},$$

$$B := \begin{bmatrix} 0 \\ \vdots \\ 0 \\ B_0 \end{bmatrix},$$

$$E := \begin{bmatrix} E_0^T & 0 & \cdots & 0 \end{bmatrix}^T, \quad C := \begin{bmatrix} 0 & \cdots & 0 & C_0 \end{bmatrix}.$$

To control the platoon, we consider state feedback control laws of the form $u = Fx$ with

$$F = \begin{bmatrix} F_N & \cdots & F_1 & F_0 \end{bmatrix},$$

where $F_i \in \mathbb{R}^{1\times 3}$. Such control law results in a closed loop

$$\begin{aligned} \dot{x} &= (A + BF)x + Ea_{N+1}, \\ a_0 &= Cx. \end{aligned} \tag{15}$$

We adopt the head-to-tail string stability notion as originally proposed in [43] (analogous notions appear, e.g. in [44]). The

[2]This is true for the proposed human-driven model for any of the parameters in Remark 1, and was also shown in [36], [37] for the optimal velocity model.

term 'head-to-tail' refers to the fact that the absence of string stability due to human-driven vehicles can be compensated by the automated vehicle at the end of the platoon.

Definition 2 (Head-to-Tail String Stability): Consider the mixed platoon described by (15)*. Let $u = Fx$ be a state feedback control law, and let $T_F(s) := C(sI - A - BF)^{-1}E$ be the closed-loop transfer function from a_{N+1} to a_0. If*

$$\|T_F(s)\|_\infty \leq 1,$$

then the control law is said to achieve head-to-tail string stability.

B. Stabilizing Automated Vehicle

Before proposing a control design to achieve head-to-tail string stability, let us discuss stability of mixed platoons.

Lemma 1 (Stability of Mixed Platoons): Assume that A_0 in (9) *is Hurwitz (equivalently,* (8) *is satisfied). Let $F = \begin{bmatrix} F_N & \cdots & F_1 & F_0 \end{bmatrix}$ with F_i arbitrary for $i = N, \ldots, 1$ and $F_0 = \begin{bmatrix} f_{01} & f_{02} & f_{03} \end{bmatrix}$. The mixed platoon* (15) *controlled by $u = Fx$ is stable if and only if f_{01}, f_{02}, f_{03} satisfy*

$$\begin{aligned} f_{03} &< 1, \\ (f_{01}h + f_{02})(1 - f_{03}) &> \tau f_{01}, \\ f_{01} &> 0. \end{aligned} \tag{16}$$

Proof: Obviously, $A+BF$ is Hurwitz if and only if A_0 and $A_1 + B_0F_0$ are Hurwitz. Since the characteristic polynomial of $A_1 + B_0F_0$ is

$$\rho(\lambda) = \lambda^3 + \frac{1 - f_{03}}{\tau}\lambda^2 + \frac{f_{01}h + f_{02}}{\tau}\lambda + \frac{f_{01}}{\tau},$$

by the Routh-Hurwitz criterion we obtain that $A_1 + B_0F_0$ is Hurwitz if and only if the conditions (16) hold. □

C. String Stabilizing Automated Vehicle

By Lemma 1, $F_N, F_{N-1}, \cdots, F_1$ do not influence stability. Therefore, one can try to design these gains to achieve string stability of the mixed platoon. The following result states that, for an appropriate choice of $F = \begin{bmatrix} F_N & F_{N-1} & \cdots & F_0 \end{bmatrix}$, the transfer function $T_F(s)$ takes a simple (third-order) form.

Theorem 2 (Reduced-Order Structure of T_F): Let $F_0 = \begin{bmatrix} f_{01} & f_{02} & f_{03} \end{bmatrix}$ be such that $A_1 + B_0F_0$ is Hurwitz. Define the gains $F_i = \begin{bmatrix} f_{i1} & f_{i2} & f_{i3} \end{bmatrix}$, $(i = N, \ldots, 1)$ as

$$\begin{aligned} f_{i1} &:= f_{01}, \\ f_{i2} &:= f_{02} - ihf_{01}, \\ f_{i3} &:= 0, \end{aligned} \tag{17}$$

Then, the closed-loop transfer function $T_F(s)$ is equal to

$$T_F(s) = \frac{(f_{02} - Nhf_{01})s + f_{01}}{\tau s^3 + (1 - f_{03})s^2 + (f_{02} + hf_{01})s + f_{01}}. \tag{18}$$

Moreover, the control action $u = Fx$ can be written as

$$\begin{aligned} u = f_{01}(s_{N+1} - s_0 - hv_0 - Nhv_{N+1}) \\ + f_{02}(v_{N+1} - v_0) + f_{03}a_0. \end{aligned} \tag{19}$$

Proof: For $i = N, \ldots, 1$, let F_i be given by (17). Define a $3 \times 3(N+1)$ matrix Π by (20), shown at the bottom of the next page.

Then, by inspection, we have

$$\begin{aligned} F &= F_0\Pi \\ \Pi(A + BF) &= (A_1 + B_0F_0)\Pi \\ C &= C_0\Pi. \end{aligned}$$

As a result, the transfer function of the closed-loop system (15) is equal to

$$\begin{aligned} C(sI - A - BF)^{-1}E &= C_0\Pi(sI - A - BF)^{-1}E \\ &= C_0(sI - A_1 - B_0F_0)^{-1}\Pi E. \end{aligned}$$

One sees that this transfer function is the transfer function of the third-order system

$$\begin{aligned} \dot{\hat{x}} &= (A_1 + B_0F_0)\hat{x} + \hat{E}a_{N+1}, \\ a_0 &= C_0\hat{x}. \end{aligned} \tag{21}$$

where $\hat{E} = \Pi E = \begin{bmatrix} -Nh & 1 & 0 \end{bmatrix}^T$, and this transfer function can be calculated to be equal to (18). Now define

$$\hat{x} = \begin{bmatrix} s_{N+1} - s_0 - hv_0 - Nhv_{N+1} \\ v_{N+1} - v_0 \\ a_0 \end{bmatrix}.$$

It can then be verified that $\hat{x} = \Pi x$. Since $F = F_0\Pi$, the control action is therefore equal to

$$u = Fx = F_0\Pi x = F_0\hat{x}$$

which is equal to (19). □

Remark 2 (Alternative Interpretation of Control Action): It is easily seen that the control action (19) can also be written as

$$\begin{aligned} u = f_{01}&(s_{N+1} - s_0 - (N+1)hv_0) \\ &+ (f_{02} - Nhf_{01})(v_{N+1} - v_0 - (N+1)ha_0) \\ &+ (f_{03} + (f_{02} - Nhf_{01})(N+1)h)a_0, \end{aligned}$$

which has a clear interpretation in terms of feedback from the spacing error between the leading and the automated vehicle, its derivative, and the acceleration of the automated vehicle.

The above shows that by choosing F as in Theorem 2, both stability and head-to-tail string stability are obtained by choosing $F_0 = \begin{bmatrix} f_{01} & f_{02} & f_{03} \end{bmatrix}$ such that $A_1 + B_0F_0$ is Hurwitz and $||\hat{T}_{F_0}(s)||_\infty \leq 1$, where $\hat{T}_{F_0}(s) = C_0(sI - A_1 - B_0F_0)^{-1}\hat{E}$. Note that, by (18), for every stabilizing F_0 we have $\hat{T}_{F_0}(0) = 1$. This means that we should aim at finding F_0 such that $||\hat{T}_{F_0}(s)||_\infty = 1$. To get close to this optimal value, we will solve a strict $\mathcal{H}_\infty$ control problem for the third-order system (21). Before this, we formulate the following theorem.

Theorem 3 ($\mathcal{H}_\infty$ Control Design for String Stability): Consider the general system

$$\begin{aligned} \dot{x} &= Ax + Bu + Ed, \\ z &= Cx, \end{aligned}$$

where $A \in \mathbb{R}^{n\times n}$, $B \in \mathbb{R}^{n\times m}$, $E \in \mathbb{R}^{n\times r}$, and $C \in \mathbb{R}^{p\times n}$. Assume B has full column rank and let $\gamma > 0$. There exists $F \in \mathbb{R}^{m\times n}$ such that $A + BF$ is Hurwitz and $||C(sI - A - BF)^{-1}E||_\infty < \gamma$ if and only if there exists $X > 0$ such that

$$\begin{bmatrix} B \\ 0 \end{bmatrix}^\perp \begin{bmatrix} AX + XA^T + \frac{1}{\gamma^2}EE^T & XC^T \\ CX & -I_p \end{bmatrix} \begin{bmatrix} B \\ 0 \end{bmatrix}^{\perp T} < 0. \tag{22}$$

In that case, a suitable F is given by

$$F = -\frac{1}{2} r B^T X^{-1} \tag{23}$$

where $r > 0$ is such that

$$\begin{bmatrix} AX + XA^T + \frac{1}{\gamma^2} EE^T - rBB^T & XC^T \\ CX & -I_p \end{bmatrix} < 0. \tag{24}$$

Proof: We refer to the Appendix. □

Now we apply Theorem 3 to the design of a suitable $F_0 = \begin{bmatrix} f_{01} & f_{02} & f_{03} \end{bmatrix}$ so that $||T_{F_0}(s)||_\infty$ is close to 1.

Indeed, take $\gamma = 1 + \epsilon$, where $\epsilon > 0$ is small. Note that $B_0 = \begin{bmatrix} 0 & 0 & \frac{1}{\tau} \end{bmatrix}^T$ and hence

$$\begin{bmatrix} B_0 \\ 0 \end{bmatrix}^\perp = \begin{bmatrix} I_2 & 0 & 0 \\ 0 & 0 & 0 \end{bmatrix}.$$

Thus, in our special case, the LMI (22) reduces to

$$\begin{bmatrix} I_2 & 0 & 0 \\ 0 & 0 & 0 \end{bmatrix} \begin{bmatrix} A_1 X + X A_1^T + \frac{1}{(1+\epsilon)^2} \hat{E}\hat{E}^T & XC_0^T \\ C_0 X & -1 \end{bmatrix} \times \begin{bmatrix} I_2 & 0 \\ 0 & 0 \\ 0 & 0 \end{bmatrix} < 0, \tag{25}$$

with $X \in \mathbb{R}^{3\times 3}$. If $X > 0$ is a solution to LMI (25), then

$$F_0 := -\frac{1}{2} r B_0^T X^{-1}, \tag{26}$$

with $r > 0$ a scalar such that

$$\begin{bmatrix} A_1 X + X A_1^T + \dfrac{1}{(1+\epsilon)^2} \hat{E}\hat{E}^T - rB_0 B_0^T & XC_0^T \\ C_0 X & -1 \end{bmatrix} < 0, \tag{27}$$

makes $A_1 + B_0 F_0$ Hurwitz and yields

$$||C_0(sI - A_1 - B_0 F_0)^{-1}\hat{E}||_\infty < 1 + \epsilon. \tag{28}$$

As compared to state-of-the-art studies on head-to-tail string stability [36], the proposed controller is found in a reduced-order way instead of using high-order numerical methods (cf. simulations in Section VI).

Remark 3 (Incremental and Scalable Structure): The proposed controller $u = \begin{bmatrix} F_N & F_{N-1} & \cdots & F_0 \end{bmatrix} x$ enjoys some incremental and scalable features. Assuming that a new vehicle (call it $N+2$) appears as the new leader in front of the platoon, the new incremental control law becomes

$$u = \begin{bmatrix} F_{N+1} & F_N & \cdots & F_0 \end{bmatrix} \begin{bmatrix} x_{N+1} \\ x \end{bmatrix}. \tag{29}$$

Two options are possible to design the gains. If (25), (26), (27) are feasible for the same F_0 as before (note that $\hat{E}$ becomes $\begin{bmatrix} -(N+1)h & 1 & 0 \end{bmatrix}^T$), then the gains $F_N \cdots F_0$ are the same as before, and the new gain F_{N+1} is directly obtained from (17), i.e., $F_{N+1} = \begin{bmatrix} f_{01} & f_{02} - (N+1)hf_{01} & 0 \end{bmatrix}$. If (25), (26), (27) are no longer feasible for the same F_0 with the new $\hat{E}$ for $N+1$, a new F_0 must be obtained and all other gains $F_{N+1} \cdots F_1$ follow from the new F_0 according to (17).

V. Safety in Head-to-Tail String Stability

Research up to now has usually approached head-to-tail string stability by solving high-dimensional $\mathcal{H}_\infty$ control problems [36], [44], [45]. The structural properties behind this have always remained hidden. The design after Theorem 3 highlights the simple structural properties of head-to-tail string stability, but also its limitations. Most importantly, the fact that the controller uses measurements only from vehicles 0 and $N+1$ (cf. (19)) poses serious problems with respect to *safety*.[3] Several notions of safety have been proposed in the literature, such as the time-to-collision and the spacing error, depending on the emphasis on emergency maneuvers or on maintaining the desired inter-vehicle distance. In this work, the *spacing error between vehicles 1 and 0* (i.e. e_0) is used as a safety measure: note that the effect of the disturbance a_{N+1} on e_0 can be characterized in terms of a transfer function.

Let us notice that considering directly the transfer function from a_{N+1} to e_0 would necessarily result in a high-order transfer function, as will be shown soon. In the following, we aim to give a reduced-order characterization of safety for our control structure, which is amenable for reduced-order control design. Consider the platoon given by (14). Starting from the reduced-order controller $u = Fx$ with $F = F_0\Pi$ obtained in Theorem 2, we propose to extend this controller as

$$\tilde{u} = F_0 \Pi x + k_{01} e_0 + k_{02} \dot{e}_0. \tag{30}$$

In other words, we consider extra feedback terms using e_0 (through k_{01}) and $\dot{e}_0 = v_1 - v_0 - ha_0$ (through k_{02}). The choice of the feedback structure (30) will be motivated by the reduced-order relation obtained before Definition 3 below.

As both e_0 and $\dot{e}_0$ can be constructed from the state x, the control law (30) can be written as

$$\tilde{u} = \tilde{F}\tilde{\Pi} x, \tag{31}$$

with $\tilde{F} := \begin{bmatrix} f_{01} & f_{02} & f_{03} & k_{01} & k_{02} \end{bmatrix}$ and a $5 \times 3(N+1)$ matrix

$$\tilde{\Pi} := \begin{bmatrix} & & & \Pi & & \\ 0 & \cdots & 0 & 1 & 0 & 0 \\ 0 & \cdots & 0 & 0 & 1 & -h \end{bmatrix}$$

with Π as in (20). Now, following a similar reasoning as in the proof of Theorem 2, we have that

$$\begin{aligned} \dot{\tilde{x}} &= \tilde{A}\tilde{x} + \tilde{B}\tilde{u} + \tilde{E}a_{N+1} + \tilde{L}a_1, \\ a_0 &= \tilde{C}\tilde{x}. \end{aligned} \tag{32}$$

[3] Simulations in Section VI will show that safety issues are intrinsic in the notion of string stability: even a full-state feedback controller designed using a high-dimensional $\mathcal{H}_\infty$ control problem poses safety issues.

$$\Pi := \begin{bmatrix} 1 & -Nh & 0 & 1 & -(N-1)h & 0 & \cdots & 1 & -h & 0 & 1 & 0 & 0 \\ 0 & 1 & 0 & 0 & 1 & 0 & \cdots & 0 & 1 & 0 & 0 & 1 & 0 \\ 0 & 0 & 0 & 0 & 0 & 0 & \cdots & 0 & 0 & 0 & 0 & 0 & 1 \end{bmatrix} \tag{20}$$

where

$$\tilde{x} := \begin{bmatrix} s_{N+1} - s_0 - hv_0 - Nhv_{N+1} \\ v_{N+1} - v_0 \\ a_0 \\ e_0 \\ \dot{e}_0 \end{bmatrix},$$

$$\tilde{E} := \begin{bmatrix} -Nh \\ 1 \\ 0 \\ 0 \\ 0 \end{bmatrix}, \quad \tilde{L} := \begin{bmatrix} 0 \\ 0 \\ 0 \\ 0 \\ 1 \end{bmatrix},$$

$$\tilde{A} := \begin{bmatrix} 0 & 1 & -h & 0 & 0 \\ 0 & 0 & -1 & 0 & 0 \\ 0 & 0 & -\frac{1}{\tau} & 0 & 0 \\ 0 & 0 & 0 & 0 & 1 \\ 0 & 0 & -1+\frac{h}{\tau} & 0 & 0 \end{bmatrix},$$

$$\tilde{B} := \begin{bmatrix} 0 \\ 0 \\ \frac{1}{\tau} \\ 0 \\ -\frac{h}{\tau} \end{bmatrix}, \quad \tilde{C}^T := \begin{bmatrix} 0 \\ 0 \\ 1 \\ 0 \\ 0 \end{bmatrix}.$$

We are interested in how a_{N+1} influences e_0. Note that we introduced e_0 explicitly as a state variable in (32). In fact,

$$e_0 = \tilde{D}\tilde{x}, \tag{33}$$

with $\tilde{D} := \begin{bmatrix} 0 & 0 & 0 & 1 & 0 \end{bmatrix}$.

Denote the transfer function from a_1 to a_0, and the transfer function from a_{N+1} to a_0 in system (32) by $\tilde{T}_{\tilde{F}_1}(s) := \tilde{C}(sI - \tilde{A} - \tilde{B}\tilde{F})^{-1}\tilde{L}$ and $\tilde{T}_{\tilde{F}_2}(s) := \tilde{C}(sI - \tilde{A} - \tilde{B}\tilde{F})^{-1}\tilde{E}$. These transfer functions can be calculated to be equal to (36), (37), shown at the bottom of the next page, respectively. However, we should consider that a_1 is not an independent exogenous input, but it depends on a_{N+1} as an effect of vehicle propagation through the whole platoon. In other words, for $i = N, \ldots, 1$ the transfer function from a_{i+1} to a_i is given by $G(s)$ as given by (12), so that the transfer function from a_{N+1} to a_1 is equal to $G^N(s)$. Therefore, the overall transfer function from a_{N+1} to a_0 is given by

$$\tilde{T}_{\tilde{F}}(s) = \tilde{T}_{\tilde{F}_2}(s) + \tilde{T}_{\tilde{F}_1}(s)G^N(s). \tag{34}$$

Clearly, due to (33), the transfer function from a_{N+1} to e_0 can be obtained similarly to (34), with $\tilde{C}$ replaced by $\tilde{D}$. In both cases we obtain a high-order transfer function.

To obtain a reduced-order characterization of safety, we put forward the notion of *safety improvement*. Safety improvement compares (in terms of a ratio) the following transfer functions

- the 'safety' transfer function $S(s)$ from a_{N+1} to e_0 stemming from the control law (19);
- the 'safety' transfer function $\tilde{S}(s)$ from a_{N+1} to e_0 obtained by applying the control law (30).

Both transfer functions are high-order and can be calculated to be equal to (38), (39), shown at the bottom of the next page. However, compared with each other, the following relation can be obtained

$$\tilde{S}(s) = H(s)S(s), \tag{35}$$

with $H(s)$ a third-order (i.e. reduced-order) transfer function given by (40), shown at the bottom of the next page.

Remark 4 (Control Structure): The fact that the transfer function $H(s)$ in (35) has reduced order is caused by two structural aspects: first, the first terms of $\tilde{S}(s)$ and $S(s)$ have the same numerator; second, the denominator of the first terms of $S(s)$ also appears as numerator of the second term of $\tilde{S}(s)$. This is thanks to the choice of the feedback structure (30).

In view of the relation between $\tilde{S}(s)$ and $S(s)$, it is natural to formalize safety improvement as the problem of finding k_{01} and k_{02} such that $\|H(s)\|_\infty < 1$. However, from (40) we have $|H(j\omega)| \to 1$ as $\omega \to \infty$, for any k_{01}, k_{02}, which implies that safety can hardly be improved at high frequency. Therefore, one may wish to introduce a low-pass filter to improve safety at low frequency. Consider the first-order low-pass filter

$$P(s) = \frac{\omega_p}{s + \omega_p}, \tag{41}$$

where $\omega_p > 0$ is the cut-off frequency of the filter. We obtain

$$H(s)P(s) = \frac{c_3 s^3 + c_2 s^2 + c_1 s + c_0}{s^4 + a_3 s^3 + a_2 s^2 + a_1 s + a_0}, \tag{42}$$

where

$$c_1 = \frac{\omega_p(f_{01}h + f_{02})}{\tau}, \; c_2 = \frac{\omega_p(1 - f_{03})}{\tau},$$
$$c_3 = \omega_p, \; c_0 = \frac{\omega_p}{\tau}, \; a_0 = \frac{(f_{01} + k_{01})h\omega_p}{\tau},$$
$$a_1 = \frac{(f_{01} + k_{01})h\omega_p + f_{01} + k_{01} + (f_{02} + k_{02})\omega_p}{\tau},$$
$$a_2 = \frac{(f_{01} + k_{01})h + f_{02} + k_{02} + \omega_p(1 - f_{03} + k_{02}h)}{\tau},$$
$$a_3 = \frac{1 - f_{03} + k_{02}h + \tau\omega_p}{\tau}.$$

Then, the following is a natural formalization of safety improvement for low frequency accelerations a_{N+1}.

Definition 3 (Head-to-Tail Safety Improvement): Consider a platoon of human-driven vehicles interacting along a string according to (11)*, followed by an automated vehicle interacting according to* (13)*, and let* (41) *be a low-pass filter. If k_{01} and k_{02} are such that*

$$\|H(s)P(s)\|_\infty < 1, \tag{43}$$

then the gains k_{01} and k_{02} are said to improve the safety of the mixed platoon for low frequency accelerations a_{N+1}.

In the following, we propose a method to find values of k_{01} and k_{02} to make $\|H(s)P(s)\|_\infty < 1$. Using the controllable canonical form, (42) can be written as

$$H(s)P(s) = \bar{C}_2(sI - \bar{A}_K)^{-1}\bar{E}, \tag{44}$$

where

$$\bar{A}_K := \begin{bmatrix} 0 & 1 & 0 & 0 \\ 0 & 0 & 1 & 0 \\ 0 & 0 & 0 & 1 \\ -a_0 & -a_1 & -a_2 & -a_3 \end{bmatrix}, \quad \bar{E} := \begin{bmatrix} 0 \\ 0 \\ 0 \\ 1 \end{bmatrix},$$

$$\bar{C}_2^T := \begin{bmatrix} c_0 \\ c_1 \\ c_2 \\ c_3 \end{bmatrix}.$$

This leads to a state-space realization of the closed loop

$$\begin{aligned} \dot{\bar{x}} &= (\bar{A} + \bar{B}K\bar{C}_1)\bar{x} + \bar{E}\bar{d} = \bar{A}\bar{x} + \bar{B}\bar{u} + \bar{E}\bar{d}, \\ \bar{y} &= \bar{C}_1\bar{x}, \\ \bar{z} &= \bar{C}_2\bar{x}, \end{aligned} \tag{45}$$

with $\bar{A}_K = \bar{A} + \bar{B}K\bar{C}_1$, obtained by applying the static output feedback $\bar{u} = K\bar{y}$, and where (46), shown at the bottom of the next page, with $f_h = f_{01}h + f_{02}$ and $K = \begin{bmatrix} k_{01} & k_{02} \end{bmatrix}$. The design steps suggested by these reduced-order formulations can be as follows: first, design f_{01}, f_{02}, f_{03} using Theorems 2 and 3, aimed at head-to-tail string stability; second, only design k_{01}, k_{02} using Theorem 4 below, aimed at safety improvement.

The safety improvement problem of Definition 3 has been transformed into a static output-feedback problem. The following theorem is a standard result on static output-feedback $\mathcal{H}_\infty$ control [53, Thm. 7.2.2] and the proof can be found therein.

Theorem 4 ($\mathcal{H}_\infty$ Control Design for Safety Improvement): Consider the general system

$$\begin{aligned} \dot{x} &= Ax + Bu + Ed, \\ y &= C_1x, \\ z &= C_2x, \end{aligned} \tag{47}$$

where $A \in \mathbb{R}^{n\times n}$, $B \in \mathbb{R}^{n\times m}$, $E \in \mathbb{R}^{n\times r}$, $C_1 \in \mathbb{R}^{q\times n}$, and $C_2 \in \mathbb{R}^{p\times n}$. Assume B has full column rank. For $\bar{\gamma} > 0$, there exists $K \in \mathbb{R}^{m\times q}$ such that $A + BKC_1$ is Hurwitz and $||C_2(sI - A - BKC_1)^{-1}E||_\infty < \bar{\gamma}$ if and only if there exist $X > 0, Y > 0$ such that

1) $\begin{bmatrix} B \\ 0 \end{bmatrix}^\perp \begin{bmatrix} AX + XA^T + EE^T & XC_2^T \\ C_2X & -\bar{\gamma}^2 I_p \end{bmatrix} \begin{bmatrix} B \\ 0 \end{bmatrix}^{\perp T} < 0,$
2) $\begin{bmatrix} C_1^T \\ 0 \end{bmatrix}^\perp \begin{bmatrix} YA + A^TY + C_2^TC_2 & YE \\ E^TY & -\bar{\gamma}^2 I_p \end{bmatrix} \begin{bmatrix} C_1^T \\ 0 \end{bmatrix}^{\perp T} < 0,$
3) $XY = \bar{\gamma}^2 I_n.$

If the above conditions hold, a suitable controller is given by

$$K = -R\Psi^T\Phi\Lambda^T(\Lambda\Phi\Lambda^T)^{-1}, \tag{48}$$

with

$$\Omega := \begin{bmatrix} YA + A^TY & YE & C_2^T \\ E^TY & -\bar{\gamma}^2 I_r & 0 \\ C_2 & 0 & -I_p \end{bmatrix},$$

$$\Psi := \begin{bmatrix} YB \\ 0 \\ 0 \end{bmatrix}, \quad \Lambda^T := \begin{bmatrix} C_1 \\ 0 \\ 0 \end{bmatrix},$$

and R a positive definite matrix such that

$$\Phi = (\Psi R\Psi^T - \Omega)^{-1} > 0. \tag{49}$$

Theorem 4 can be applied to find a gain $K = \begin{bmatrix} k_{01} & k_{02} \end{bmatrix}$ such that $\|H(s)P(s)\|_\infty < 1$ by taking $\bar{\gamma} = 1$, $A = \bar{A}$, $B = \bar{B}$, $E = \bar{E}$, $C_1 = \bar{C}_1$, $C_2 = \bar{C}_2$. An algorithm for solving static output-feedback problems in this form is in [54].

Remark 5 (String Stability and Safety Co-Design): We have shown that by introducing two auxiliary state variables in the control law, we can define a safety improvement measure in terms of the ratio between the two transfer functions ($S(s)$ in (38) and $\tilde{S}(s)$ in (39)). This problem is also of reduced order (third order or more, depending on the introduction of a frequency-shaping filter). However, it is still an *open problem* to attain head-to-tail string stability and safety while at the same time keeping the problem of reduced order. This is essentially due to the presence of the high-order transfer function $G^N(s)$ from $a_{N+1}(s)$ to $a_1(s)$ in the system (32), whose effect cannot be removed from (34) if $k_{01}, k_{02} \neq 0$.

VI. Simulations

To validate the proposed design and compare it with standard (full-order) design, in this section we will perform numerical simulations using the parameters $b = 0.12, c = 0.4, \tau = 0.1, h = 5/3$ [36]. Two designs will be considered: both designs are in state-feedback form $u = Fx$, $F = \begin{bmatrix} F_N & F_{N-1} & \cdots & F_0 \end{bmatrix} \in \mathbb{R}^{3(N+1)}$ and aim at achieving head-to-tail string stability ($\mathcal{H}_\infty$ norm of the transfer function from a_{N+1} to a_0 less than or equal to 1). What changes is the way F is obtained:

1) Full-order design: similarly as in [36], the full-order platoon model (14) is used to get F. This is a $\mathcal{H}_\infty$ control problem as in (22)-(24) in Theorem 3, of order $3(N + 1)$;

$$\tilde{T}_{\tilde{F}_1}(s) = \frac{k_{02}s + k_{01}}{\tau s^3 + (1 - f_{03} + k_{02}h)s^2 + ((f_{01} + k_{01})h + f_{02} + k_{02})s + f_{01} + k_{01}} \tag{36}$$

$$\tilde{T}_{\tilde{F}_2}(s) = \frac{(f_{02} - Nhf_{01})s + f_{01}}{\tau s^3 + (1 - f_{03} + k_{02}h)s^2 + ((f_{01} + k_{01})h + f_{02} + k_{02})s + f_{01} + k_{01}} \tag{37}$$

$$S(s) = \frac{(hs+1)((Nhf_{01} - f_{02})s - f_{01})}{s^2(\tau s^3 + (1 - f_{03})s^2 + (f_{01}h + f_{02})s + f_{01})} + \frac{1}{s^2}G^N(s) \tag{38}$$

$$\begin{aligned} \tilde{S}(s) = {} & \frac{(hs+1)((Nhf_{01} - f_{02})s - f_{01})}{s^2(\tau s^3 + (1 - f_{03} + k_{02}h)s^2 + ((f_{01} + k_{01})h + f_{02} + k_{02})s + f_{01} + k_{01})} \\ & + \frac{(\tau s^3 + (1 - f_{03})s^2 + (f_{01}h + f_{02})s + f_{01})}{s^2(\tau s^3 + (1 - f_{03} + k_{02}h)s^2 + ((f_{01} + k_{01})h + f_{02} + k_{02})s + f_{01} + k_{01})}G^N(s) \end{aligned} \tag{39}$$

$$H(s) = \frac{\tau s^3 + (1 - f_{03})s^2 + (f_{01}h + f_{02})s + f_{01}}{\tau s^3 + (1 - f_{03} + k_{02}h)s^2 + ((f_{01} + k_{01})h + f_{02} + k_{02})s + f_{01} + k_{01}}. \tag{40}$$

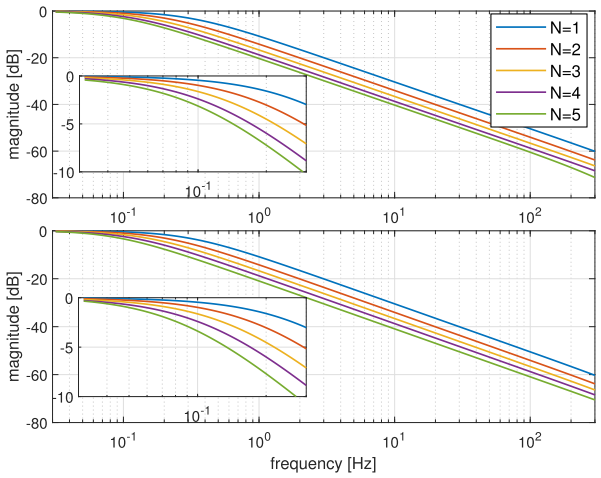

Fig. 2. Bode diagrams (magnitude) of the transfer functions from a_{N+1} to a_0: full-order design (upper), reduced-order design (lower). A zoomed Bode diagram is provided in the small plot.

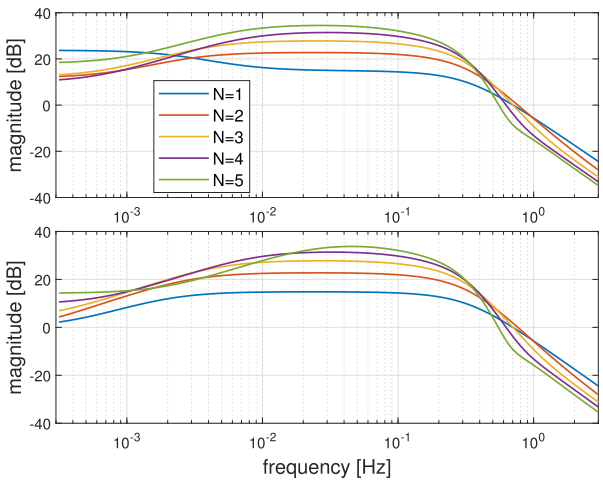

Fig. 3. Bode diagrams (magnitude) of the transfer functions from a_{N+1} to e_0: full-order design (upper), reduced-order design (lower).

2) Reduced-order design: here, F_0 is obtained by solving the $\mathcal{H}_\infty$ control problem of order 3 stemming from the LMIs (25)-(27), whereas $\begin{bmatrix} F_N & F_{N-1} & \cdots & F_1 \end{bmatrix}$ is designed according to (17) in Theorem 2.

The corresponding LMIs are implemented and solved in Matlab R2019b, using Yalmip as editor [55] and Sedumi as semidefinite programming solver [56].

A. Frequency-Domain Linear validation

For the resulting design, we will plot the transfer function from a_{N+1} to a_0 (that indicates string stability) and the transfer function from a_{N+1} to e_0 (that indicates safety). The design is performed for $N = 1, \ldots, 5$.

The magnitude of the 'string stability' transfer functions from a_{N+1} to a_0 is reported in Fig. 2, both for the full-order design (upper) and for the reduced-order design (lower). For both designs, the magnitude does not exceed 1 (0 dB), i.e., head-to-tail string stability is achieved. In addition, the magnitude plots are very close for the two designs.

The magnitude of the 'safety' transfer functions from a_{N+1} to e_0 is reported in Fig. 3, both for the full-order design (upper) and for the reduced-order design (lower). Except for the low frequency behavior for $N = 1$, both designs lead to very similar magnitude plots. Also note that the plots exhibit a peak that becomes larger as N increases. This indicates that safety decreases as N increases. In particular,

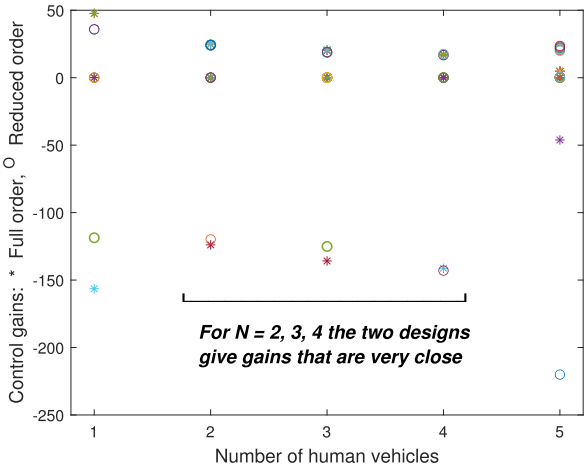

Fig. 4. Control gains of the state feedback controller $u = Fx$ as a function of N: full-order design (stars), reduced-order design (circles).

- Peaks for full-order design: 23.67 dB ($N = 1$), 22.75 dB ($N = 2$), 27.78 dB ($N = 3$), 31.42 dB ($N = 4$), 34.48 dB ($N = 5$);
- Peaks for reduced-order design: 14.82 dB ($N = 1$), 22.74 dB ($N = 2$), 27.76 dB ($N = 3$), 31.39 dB ($N = 4$), 33.75 dB ($N = 5$);

Comparing these peaks suggests that the proposed reduced-order design will not necessarily sacrifice safety as compared to the full-order design.

Fig. 4 reports all the gains in F of the state feedback controller $u = Fx$ for the full-order design (stars) and for

$$\bar{A} := \begin{bmatrix} 0 & 1 & 0 & 0 \\ 0 & 0 & 1 & 0 \\ 0 & 0 & 0 & 1 \\ -\dfrac{\omega_p f_{01} h}{\tau} & -\dfrac{f_{01} + f_h \omega_p}{\tau} & -\dfrac{(1 - f_{03})\omega_p + f_h}{\tau} & -\dfrac{1 - f_{03} + \tau \omega_p}{\tau} \end{bmatrix},$$

$$\bar{B} := \begin{bmatrix} 0 \\ 0 \\ 0 \\ -\dfrac{1}{\tau} \end{bmatrix}, \quad \bar{C}_1 := \begin{bmatrix} \omega_p & 1 + h\omega_p & h & 0 \\ 0 & \omega_p & 1 + h\omega_p & h \end{bmatrix}, \tag{46}$$

the reduced-order design (circles). Remarkably, especially for $N = 2, 3, 4$, the gains of the two designs are close to each other. For example:

Gains for full-order design with $N = 4$:

$$F = [\underbrace{0.1254\ 16.5281\ 0.0030}_{F_4}\ \underbrace{0.1257\ 16.7384\ 0.0013}_{F_3}\ \underbrace{0.1257\ 16.9489\ 0.0008}_{F_2}\ \underbrace{0.1260\ 17.1618\ -0.0054}_{F_1}\ \underbrace{0.1253\ 17.3773\ -141.2617}_{F_0}];$$

Gains for reduced-order design with $N = 4$:

$$F = [\underbrace{0.1416\ 16.6687\ 0}_{F_4}\ \underbrace{0.1416\ 16.9048\ 0}_{F_3}\ \underbrace{0.1416\ 17.1408\ 0}_{F_2}\ \underbrace{0.1416\ 17.3769\ 0}_{F_1}\ \underbrace{0.1416\ 17.6130\ -142.9814}_{F_0}];$$

Two aspects can be noticed: first, the gains of the full-order design corresponding to $f_{i1}, i = N, \ldots, 1$ are almost identical; second, the gains of the full-order design corresponding to f_{i3}, $i = N, \ldots, 1$ are not only almost identical, but also close to zero as in the reduced-order design (cf. Theorem 2).

To further highlight the trade-off between string stability and safety we consider $N = 5$ which, according to Fig. 4, is the case where the gains differ the most. The safety improvement can be demonstrated as follows: in the plane formed by the pair (k_{01}, k_{02}), we show how these gains improve safety while possibly maintaining string stability. The safety improvement is visualized by the level sets that indicate how much the safety peak of $S(s)$ (also reported in Fig. 3) is reduced by adding the gains k_{01}, k_{02}. In other words, the level sets represent the ratio between the peak of $S(s)$ in (38) (without k_{01}, k_{02}) and the peak of $\tilde{S}(s)$ in (39) (with k_{01}, k_{02}).

The results are in Figs. 5 and 6, for the full-order and reduced-order design, respectively. Remarkably, despite the different size of the regions, both designs exhibit similar trade-offs. In particular, when the level set is close to 9, i.e. the peak of $\tilde{S}(s)$ is 9 times smaller than the peak of $S(s)$ (safety is improved), both designs will go outside the region of string stability. These numerical results confirm that the performance of the proposed design is close to the performance obtained via full-order $\mathcal{H}_\infty$ control design.

B. Time-Domain Nonlinear validation

We finally report the results of our simulations using the nonlinear human-driver behavior (1)-(2) with $d_l = 5$ m, $d_u = 35$ m, $v_{\max} = 30$ m/s. In addition, to use the same parameters in [36] $b = 0.12, c = 0.4, \tau = 0.1, h = 5/3$, we calculate $\alpha = bh = 0.2$, $\beta = c = 0.4$. To capture the desired spacing corresponding to $h = 5/3$, we calculate the derivative of $V_d(d)$ with respect to d and obtain the equilibrium values $d^* = 31.3$ m and $v^* = 28.9$ m/s. We let a mixed platoon with $N = 4$ run at these equilibrium values: next, in order to simulate a safety scenario, we let the leading vehicle brake to 17 m/s. Also, to simulate a communication network environment, we make use of the TrueTime toolbox

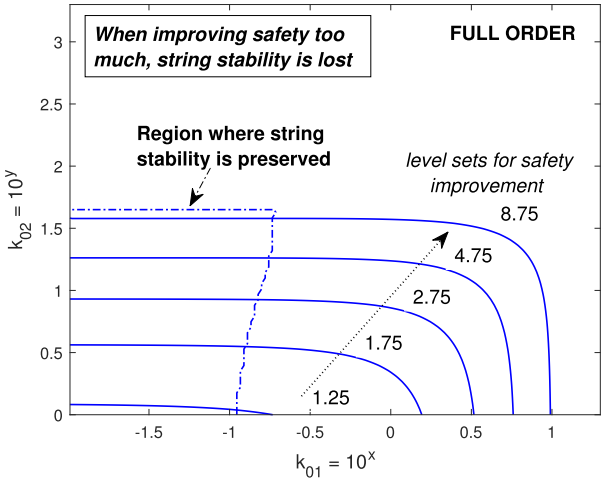

Fig. 5. String stability/safety trade-offs for $N = 5$ and full-order design as a function of k_{01}, k_{02} (in $\log_{10}$ scale): the dash-dot line represents the region in which string stability is preserved; the solid lines represent the level sets quantifying safety improvement (ratio of the peaks of $\tilde{S}(s)$ and $S(s)$).

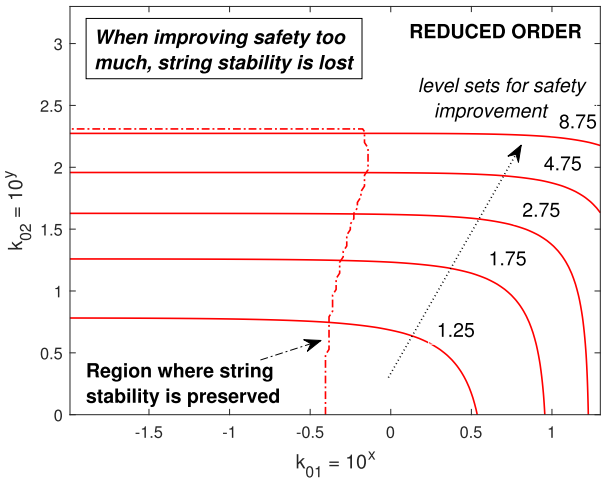

Fig. 6. String stability/safety trade-offs for $N = 5$ and reduced-order design as a function of k_{01}, k_{02} (in $\log_{10}$ scale): the dash-dot line represents the region in which string stability is preserved; the solid lines represent the level sets quantifying safety improvement (ratio of the peaks of $\tilde{S}(s)$ and $S(s)$).

developed by Lund University [57], which simulates the IEEE 802.11p wireless communication protocol. We consider four scenarios:

- Full-order design $u = Fx$ with the gains F reported in Section VI-A;
- Full-order design $u = Fx + k_{01}e_{01} + k_{02}\dot{e}_{01}$ with the same F and $k_{01} = 0.3$, $k_{02} = 100$;
- Reduced-order design $u = Fx$ with the gains F reported in Section VI-A;
- Reduced-order design $u = Fx + k_{01}e_{01} + k_{02}\dot{e}_{01}$ with the same F and $k_{01} = 0.3$, $k_{02} = 100$.

Because the full-order and the reduced-order design give almost the same results, we only report the reduced-order design, in Fig. 7 (without k_{01}, k_{02}) and in Fig. 8 (with k_{01}, k_{02}). The first figure shows a collision of the automated vehicle (AV0) with the preceding vehicle (HV1). This supports the idea that a design, even full-order, merely based on head-to-tail string stability cannot guarantee safety. When applying the feedback gains k_{01}, k_{02}, collision is avoided. This is done at

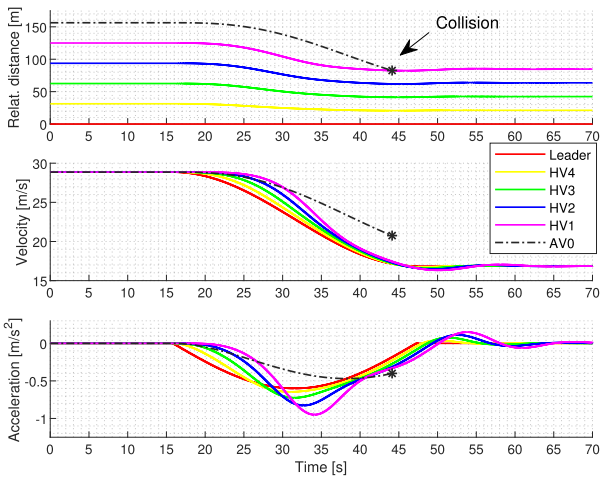

Fig. 7. Relative distance, velocity and acceleration of a mixed platoon with $N = 4$: reduced-order design without applying the gains k_{01}, k_{02} (the full-order design gives the same behavior). The relative distance is with respect to the leading vehicle. Note the collision at around $t = 45$s.

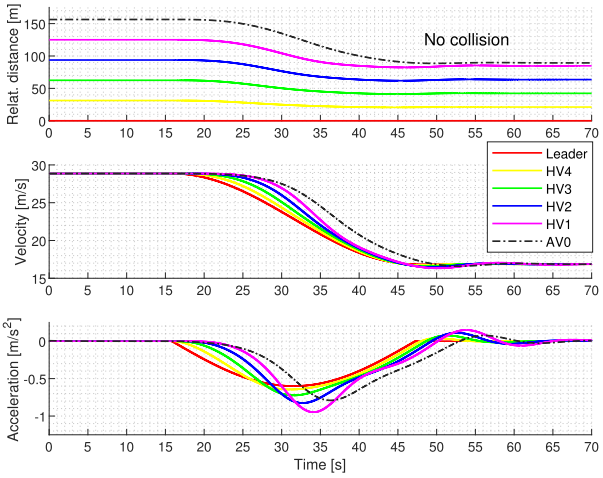

Fig. 8. Relative distance, velocity and acceleration of a mixed platoon with $N = 4$: reduced-order design with gains k_{01}, k_{02} (the full-order design gives the same behavior). The relative distance is with respect to the leading vehicle. Note that no collision occurs in this case.

the price of having a negative peak in the acceleration of AV0 at around $t = 50$s in Fig. 8, which is absent in Fig. 7. This confirms that fundamental trade-offs exist between head-to-tail string stability and safety. Let us mention that, although our theoretical analysis does not explicitly take into account the communication effects modelled by TrueTime, we have verified that the same scenarios occur when communication is ideal. In particular, the collision in Fig. 7 occurs also in case of ideal communication, while collision is avoided for the scenario in Fig. 8. It is natural to expect that the presence of increasing communication impairments cannot be beneficial to any platooning algorithm nor improve its safety.

VII. Conclusion

This paper has introduced a reduced-order theoretical framework for the problem of head-to-tail string stability of mixed (human/automated) platoons: a reduced-order design strategy has been given for head-to-tail string stability only depending on three gains. To address the safety limitations of the head-to-tail string stability notion, a reduced-order design for attaining safety improvements has been given only depending on two gains. It was shown via numerical simulations that the string stability/safety trade-offs of the proposed reduced-order design are comparable with those resulting from full-order designs.

The framework can be further investigated in several directions: an interesting one is to study if analogous structural properties apply to different vehicle-following models, such as the intelligent driving model. Another point of practical interest to include delays such as actuation delay, human reaction time and communication delay; we expect that the presence of these delays would further highlight the issue of string instability and the trade-offs with safety. The presence of heterogeneous behavior in the human-driven vehicles is another point of practical interest. Studying these practical aspects may provide insights for implementation of this approach in event-driven traffic simulators.

Appendix

This Appendix will prove Theorem 3. To do this, we first present a technical lemma (see also Theorem 2.3.12 in [53]).

Lemma 2: Assume matrix $\Gamma \in \mathbb{R}^{n\times m}$ has full column rank, matrix $\Theta \in \mathbb{R}^{n\times n}$ is symmetric, $F \in \mathbb{R}^{m\times n}$. Then, the linear matrix inequality (LMI)

$$\Theta + \Gamma F + (\Gamma F)^T < 0 \tag{50}$$

has a solution F if and only if

$$\Gamma^{\perp}\Theta\Gamma^{\perp^T} < 0. \tag{51}$$

If (51) holds, then a solution F is given by

$$F = -\frac{1}{2}r\Gamma^T,$$

where $r > 0$ is such that

$$\Theta - r\Gamma\Gamma^T < 0. \tag{52}$$

Proof: Since Γ has full column rank, $\Gamma^{\perp}$ is well defined and has full row rank.

Necessity. Assume (50) has a solution F. Then

$$\Gamma^{\perp}(\Theta + \Gamma F + F^T\Gamma^T)\Gamma^{\perp^T} < 0,$$

which implies $\Gamma^{\perp}\Theta\Gamma^{\perp^T} < 0$.

Sufficiency. Assume $\Gamma^{\perp}\Theta\Gamma^{\perp^T} < 0$. By Finsler's Lemma [53], there exist a $r > 0$ such that

$$\Theta - r\Gamma\Gamma^T < 0$$

Define $F = -\frac{1}{2}r\Gamma^T$, it is easy to verify that F indeed satisfies (50). □

We are now in the position to prove Theorem 3 in the framework of bounded real lemma [53]. *Proof:* By the bounded real lemma, having $||C(sI - A - BF)^{-1}E||_{\infty} < \gamma$ is equivalent to the existence of $Y > 0$ such that

$$Y(A + BF) + (A + BF)^T Y + \frac{1}{\gamma^2}YEE^TY + C^TC < 0 \tag{53}$$

Denote

$$\Theta := YA + A^TY + \frac{1}{\gamma^2}YEE^TY + C^TC,$$
$$\Gamma := YB.$$

Obviously, (53) can be rewritten in the form (50). Therefore, by Lemma 2, inequality (53) has a solution if and

only if

$$B^{\perp}Y^{-1}(YA + A^TY + \frac{1}{\gamma^2}YEE^TY + C^TC)Y^{-1}B^{\perp^T} < 0$$

equivalently,

$$B^{\perp}(AY^{-1} + Y^{-1}A^T + \frac{1}{\gamma^2}EE^T + Y^{-1}C^TCY^{-1})B^{\perp^T} < 0 \tag{54}$$

Denote $X := Y^{-1}$. Then, (54) holds if and only if

$$\begin{bmatrix} B \\ 0 \end{bmatrix}^{\perp} \begin{bmatrix} AX + XA^T + \frac{1}{\gamma^2}EE^T & XC^T \\ CX & -I_p \end{bmatrix} \begin{bmatrix} B \\ 0 \end{bmatrix}^{\perp^T} < 0$$

The proof is concluded by noticing that (52) leads to (24). □

REFERENCES

[1] L. E. Peppard, "String stability of relative-motion PID vehicle control systems," *IEEE Trans. Autom. Control*, vol. AC-19, no. 5, pp. 579–581, Oct. 1974.

[2] D. Swaroop and J. K. Hedrick, "String stability of interconnected systems," *IEEE Trans. Autom. Control*, vol. 41, no. 3, pp. 349–357, Mar. 1996.

[3] J. Ploeg, N. van de Wouw, and H. Nijmeijer, "Lp string stability of cascaded systems: Application to vehicle platooning," *IEEE Trans. Control Syst. Technol.*, vol. 22, no. 2, pp. 786–793, Mar. 2014.

[4] A. Pant, P. Seiler, and K. Hedrick, "Mesh stability of look-ahead interconnected systems," *IEEE Trans. Autom. Control*, vol. 47, no. 2, pp. 403–407, Feb. 2002.

[5] I. Herman, S. Knorn, and A. Ahlén, "Disturbance scaling in bidirectional vehicle platoons with different asymmetry in position and velocity coupling," *Automatica*, vol. 82, pp. 13–20, Aug. 2017.

[6] S. Knorn, A. Donaire, J. C. Agüero, and R. H. Middleton, "Scalability of bidirectional vehicle strings with static and dynamic measurement errors," *Automatica*, vol. 62, pp. 208–212, Dec. 2015.

[7] C. Cai and G. Hagen, "Stability analysis for a string of coupled stable subsystems with negative imaginary frequency response," *IEEE Trans. Autom. Control*, vol. 55, no. 8, pp. 1958–1963, Aug. 2010.

[8] R. H. Middleton and J. H. Braslavsky, "String instability in classes of linear time invariant formation control with limited communication range," *IEEE Trans. Autom. Control*, vol. 55, no. 7, pp. 1519–1530, Jul. 2010.

[9] A. Petrillo, A. Pescapé, and S. Santini, "A secure adaptive control for cooperative driving of autonomous connected vehicles in the presence of heterogeneous communication delays and cyberattacks," *IEEE Trans. Cybern.*, vol. 51, no. 3, pp. 1134–1149, Jan. 2020.

[10] A. Sarker *et al.*, "A review of sensing and communication, human factors, and controller aspects for information-aware connected and automated vehicles," *IEEE Trans. Intell. Transp. Syst.*, vol. 21, no. 1, pp. 7–29, Jan. 2020.

[11] S. Feng, Y. Zhang, S. E. Li, Z. Cao, H. X. Liu, and L. Li, "String stability for vehicular platoon control: Definitions and analysis methods," *Annu. Rev. Control*, vol. 47, pp. 81–97, Mar. 2019.

[12] B. Besselink and K. H. Johansson, "String stability and a delay-based spacing policy for vehicle platoons subject to disturbances," *IEEE Trans. Autom. Control*, vol. 62, no. 9, pp. 4376–4391, Sep. 2017.

[13] M. Barreau, A. Seuret, F. Gouaisbaut, and L. Baudouin, "Lyapunov stability analysis of a string equation coupled with an ordinary differential system," *IEEE Trans. Autom. Control*, vol. 63, no. 11, pp. 3850–3857, Nov. 2018.

[14] G. Rödönyi, "Heterogeneous string stability of unidirectionally interconnected MIMO LTI systems," *Automatica*, vol. 103, pp. 354–362, May 2019.

[15] J. Monteil, M. Bouroche, and D. J. Leith, "L_2 and L_∞ stability analysis of heterogeneous traffic with application to parameter optimization for the control of automated vehicles," *IEEE Trans. Control Syst. Technol.*, vol. 27, no. 3, pp. 934–949, May 2019.

[16] D. Liu, S. Baldi, V. Jain, W. Yu, and P. Frasca, "Cyclic communication in adaptive strategies to platooning: The case of synchronized merging," *IEEE Trans. Intell. Vehicles*, vol. 6, no. 3, pp. 490–500, Sep. 2021.

[17] A. Bayuwindra, J. Ploeg, E. Lefeber, and H. Nijmeijer, "Combined longitudinal and lateral control of car-like vehicle platooning with extended look-ahead," *IEEE Trans. Control Syst. Technol.*, vol. 28, no. 3, pp. 790–803, May 2020.

[18] P. Wijnbergen and B. Besselink, "Existence of decentralized controllers for vehicle platoons: On the role of spacing policies and available measurements," *Syst. Control Lett.*, vol. 145, Nov. 2020, Art. no. 104796.

[19] P. Seiler, A. Pant, and K. Hedrick, "Disturbance propagation in vehicle strings," *IEEE Trans. Autom. Control*, vol. 49, no. 10, pp. 1835–1842, Oct. 2004.

[20] A. Farnam and A. Sarlette, "Toward a comprehensive impossibility result for string stability," *IEEE Trans. Autom. Control*, vol. 65, no. 4, pp. 1652–1659, Apr. 2020.

[21] G. Gunter *et al.*, "Are commercially implemented adaptive cruise control systems string stable," *IEEE Trans. Intell. Transp. Syst.*, vol. 22, no. 11, pp. 6992–7003, Nov. 2021.

[22] M. Bando, K. Hasebe, A. Nakayama, A. Shibata, and Y. Sugiyama, "Dynamical model of traffic congestion and numerical simulation," *Phys. Rev. E, Stat. Phys. Plasmas Fluids Relat. Interdiscip. Top.*, vol. 51, pp. 1035–1042, Feb. 1995.

[23] M. Treiber, A. Hennecke, and D. Helbing, "Congested traffic states in empirical observations and microscopic simulations," *Phys. Rev. E, Stat. Phys. Plasmas Fluids Relat. Interdiscip. Top.*, vol. 62, no. 2, pp. 1805–1824, 2000.

[24] W. Zhao, D. Ngoduy, S. Shepherd, R. Liu, and M. Papageorgiou, "A platoon based cooperative eco-driving model for mixed automated and human-driven vehicles at a signalised intersection," *Transp. Res. C, Emerg. Technol.*, vol. 95, pp. 802–821, Oct. 2018.

[25] R. Yan, D. Yang, B. Wijaya, and C. Yu, "Feedforward compensation-based finite-time traffic flow controller for intelligent connected vehicle subject to sudden velocity changes of leading vehicle," *IEEE Trans. Intell. Transp. Syst.*, vol. 21, no. 8, pp. 3357–3365, Aug. 2020.

[26] A. Kesting and M. Treiber, "How reaction time, update time, and adaptation time influence the stability of traffic flow," *Comput.-Aided Civil Infrastruct. Eng.*, vol. 23, no. 2, pp. 125–137, 2008.

[27] Y. Sugiyama *et al.*, "Traffic jams without bottlenecks—Experimental evidence for the physical mechanism of the formation of a jam," *New J. Phys.*, vol. 10, no. 3, Mar. 2008, Art. no. 033001.

[28] S. Stüdli, M. M. Seron, and R. H. Middleton, "Vehicular platoons in cyclic interconnections," *Automatica*, vol. 94, pp. 283–293, Aug. 2018.

[29] J. Zhou and F. Zhu, "Modeling the fundamental diagram of mixed human-driven and connected automated vehicles," *Transp. Res. C, Emerg. Technol.*, vol. 115, Jun. 2020, Art. no. 102614.

[30] F. Zhu and S. V. Ukkusuri, "An optimal estimation approach for the calibration of the car-following behavior of connected vehicles in a mixed traffic environment," *IEEE Trans. Intell. Transp. Syst.*, vol. 18, no. 2, pp. 282–291, Feb. 2017.

[31] V. Punzo, Z. Zheng, and M. Montanino, "About calibration of car-following dynamics of automated and human-driven vehicles: Methodology, guidelines and codes," *Transp. Res. C, Emerg. Technol.*, vol. 128, Jul. 2021, Art. no. 103165.

[32] R. E. Stern *et al.*, "Dissipation of stop-and-go waves via control of autonomous vehicles: Field experiments," *Transp. Res. C, Emerg. Technol.*, vol. 89, pp. 205–221, Apr. 2018.

[33] J. Sun, Z. Zheng, and J. Sun, "Stability analysis methods and their applicability to car-following models in conventional and connected environments," *Transp. Res. B, Methodol.*, vol. 109, pp. 212–237, Mar. 2018.

[34] X. Chang, H. Li, J. Rong, X. Zhao, and A. Li, "Analysis on traffic stability and capacity for mixed traffic flow with platoons of intelligent connected vehicles," *Phys. A, Stat. Mech. Appl.*, vol. 557, Nov. 2020, Art. no. 124829.

[35] Y. Zheng, J. Wang, and K. Li, "Smoothing traffic flow via control of autonomous vehicles," *IEEE Internet Things J.*, vol. 7, no. 5, pp. 3882–3896, May 2020.

[36] D. Hajdu, J. I. Ge, T. Insperger, and G. Orosz, "Robust design of connected cruise control among human-driven vehicles," *IEEE Trans. Intell. Transp. Syst.*, vol. 21, no. 2, pp. 749–761, Feb. 2020.

[37] V. Giammarino, S. Baldi, P. Frasca, and M. L. D. Monache, "Traffic flow on a ring with a single autonomous vehicle: An interconnected stability perspective," *IEEE Trans. Intell. Transp. Syst.*, vol. 22, no. 8, pp. 4998–5008, Aug. 2021.

[38] J. I. Ge and G. Orosz, "Optimal control of connected vehicle systems with communication delay and driver reaction time," *IEEE Trans. Intell. Transp. Syst.*, vol. 18, no. 8, pp. 2056–2070, Aug. 2017.

[39] J. Wang, Y. Zheng, Q. Xu, J. Wang, and K. Li, "Controllability analysis and optimal control of mixed traffic flow with human-driven and autonomous vehicles," *IEEE Trans. Intell. Transp. Syst.*, vol. 22, no. 12, pp. 7445–7459, Dec. 2021.

[40] M. Di Vaio, G. Fiengo, A. Petrillo, A. Salvi, S. Santini, and M. Tufo, "Cooperative shock waves mitigation in mixed traffic flow environment," *IEEE Trans. Intell. Transp. Syst.*, vol. 20, no. 12, pp. 4339–4353, Dec. 2019.
[41] J. Sun, Z. Zheng, and J. Sun, "The relationship between car following string instability and traffic oscillations in finite-sized platoons and its use in easing congestion via connected and automated vehicles with IDM based controller," *Transp. Res. B, Methodol.*, vol. 142, pp. 58–83, Dec. 2020.
[42] J. Monteil, G. Russo, and R. Shorten, "On L_∞ string stability of nonlinear bidirectional asymmetric heterogeneous platoon systems," *Automatica*, vol. 105, pp. 198–205, Jul. 2019.
[43] J. I. Ge and G. Orosz, "Dynamics of connected vehicle systems with delayed acceleration feedback," *Transp. Res. C, Emerg. Technol.*, vol. 46, pp. 46–64, Sep. 2014.
[44] F. Li and Y. Wang, "Cooperative adaptive cruise control for string stable mixed traffic: Benchmark and human-centered design," *IEEE Trans. Intell. Transp. Syst.*, vol. 18, no. 12, pp. 3473–3485, Dec. 2017.
[45] Y. Zhou, S. Ahn, M. Wang, and S. Hoogendoorn, "Stabilizing mixed vehicular platoons with connected automated vehicles: An H-infinity approach," *Transp. Res. B, Methodol.*, vol. 132, pp. 152–170, Feb. 2020.
[46] S. Sheikholeslam and C. A. Desoer, "Longitudinal control of a platoon of vehicles with, no., communication of lead vehicle information: A system level study," *IEEE Trans. Veh. Technol.*, vol. 42, no. 4, pp. 546–554, Nov. 1993.
[47] G. C. Goodwin, S. F. Graebe, and M. E. Salgado, *Control Systems Design*. Upper Saddle River, NJ, USA: Prentice-Hall, 2001.
[48] L. Zhang, J. Sun, and G. Orosz, "Hierarchical design of connected cruise control in the presence of information delays and uncertain vehicle dynamics," *IEEE Trans. Control Syst. Technol.*, vol. 26, no. 1, pp. 139–150, Jan. 2018.
[49] J. I. Ge and G. Orosz, "Connected cruise control among human-driven vehicles: Experiment-based parameter estimation and optimal control design," *Transp. Res. C, Emerg. Technol.*, vol. 95, pp. 445–459, Oct. 2018.
[50] S. Baldi, D. Liu, V. Jain, and W. Yu, "Establishing platoons of bidirectional cooperative vehicles with engine limits and uncertain dynamics," *IEEE Trans. Intell. Transp. Syst.*, vol. 22, no. 5, pp. 2679–2691, May 2021.
[51] J. C. Zegers, E. Semsar-Kazerooni, J. Ploeg, N. van de Wouw, and H. Nijmeijer, "Consensus control for vehicular platooning with velocity constraints," *IEEE Trans. Control Syst. Technol.*, vol. 26, no. 5, pp. 1592–1605, Sep. 2018.
[52] W. B. Qin and G. Orosz, "Experimental validation of string stability for connected vehicles subject to information delay," *IEEE Trans. Control Syst. Technol.*, vol. 28, no. 4, pp. 1203–1217, Jul. 2020.
[53] R. E. Skelton, T. Iwasaki, and D. E. Grigoriadis, *A Unified Algebraic Approach to Control Design*. Boca Raton, FL, USA: CRC Press, 1997.
[54] L. El Ghaoui, F. Oustry, and M. AitRami, "A cone complementarity linearization algorithm for static output-feedback and related problems," *IEEE Trans. Autom. Control*, vol. 42, no. 8, pp. 1171–1176, Aug. 1997.
[55] J. Lofberg, "YALMIP: A toolbox for modeling and optimization in MATLAB," in *Proc. IEEE Int. Conf. Robot. Autom.*, Sep. 2004, pp. 284–289.
[56] J. Sturm, "Using SeDuMi 1.02, a MATLAB toolbox for optimization over symmetric cones," *Optim. Methods Softw.*, vols. 11–12, nos. 1–4, pp. 625–653, 1999. [Online]. Available: http://fewcal.kub.nl/sturm
[57] A. Cervin, D. Henriksson, B. Lincoln, J. Eker, and K.-E. Årzén, "How does control timing affect performance? Analysis and simulation of timing using Jitterbug and TrueTime," *IEEE Control Syst. Mag.*, vol. 23, no. 3, pp. 16–30, Jun. 2003.

Di Liu (Member, IEEE) received the B.Sc. degree in information science from the Hubei University of Science and Technology, China, in 2014, the M.Sc. degree in control science and engineering from the Chongqing University of Posts and Telecommunications, China, in 2017, and the Ph.D. degree in cyber science and engineering from Southeast University, Nanjing, China, in 2021. She is currently pursuing the second Ph.D. degree with the Bernoulli Institute for Mathematics, Computer Science and Artificial Intelligence, University of Groningen, The Netherlands. Her research interests are learning systems and control, with application in intelligent transportation, automated vehicles, and unmanned aerial vehicles.

Bart Besselink (Member, IEEE) received the M.Sc. degree *(cum laude)* in mechanical engineering and the Ph.D. degree from the Eindhoven University of Technology, The Netherlands, in 2008 and 2012, respectively. He was a Visiting Researcher with the Tokyo Institute of Technology, Japan, in 2012. From 2012 to 2016, he was a Post-Doctoral Researcher with the ACCESS Linnaeus Center and the Department of Automatic Control, KTH Royal Institute of Technology, Stockholm, Sweden. Since 2016, he has been an Assistant Professor with the Bernoulli Institute for Mathematics, Computer Science and Artificial Intelligence, University of Groningen, The Netherlands. His main research interests include systems theory and model reduction for nonlinear dynamical systems and large-scale interconnected systems.

Simone Baldi (Senior Member, IEEE) received the B.Sc. degree in electrical engineering and the M.Sc. and Ph.D. degrees in control systems engineering from the University of Florence, Italy, in 2005, 2007, and 2011, respectively. He is currently a Professor at the School of Mathematics, Southeast University, with a guest position at the Delft Center for Systems and Control, TU Delft, where he was an Assistant Professor. His research interests include adaptive and learning systems with applications in networked control and intelligent vehicles. He is a Subject Editor of the *International Journal of Adaptive Control and Signal Processing* and an Associate Editor of IEEE CONTROL SYSTEMS LETTERS.

Wenwu Yu (Senior Member, IEEE) received the B.Sc. degree in information and computing science and the M.Sc. degree in applied mathematics from Southeast University, Nanjing, China, in 2004 and 2007, respectively, and the Ph.D. degree in electronic engineering from the City University of Hong Kong, Hong Kong, China, in 2010. He is currently the Founding Director of the Laboratory of Cooperative Control of Complex Systems, the Deputy Associate Director of the Jiangsu Provincial Key Laboratory of Networked Collective Intelligence, and a Full Professor with the Endowed Chair Honor, Southeast University. His research interests include multi-agent systems, complex networks and systems, disturbance control, distributed optimization, machine learning, smart grids, and intelligent transportation systems. He serves as an Editorial Board Member for several flag journals, including IEEE TRANSACTIONS ON CIRCUITS AND SYSTEMS—II: EXPRESS BRIEFS, IEEE TRANSACTIONS ON INDUSTRIAL INFORMATICS, IEEE TRANSACTIONS ON SYSTEMS, MAN, AND CYBERNETICS: SYSTEMS, *Science China Information Sciences*, and *Science China Technological Sciences*. He was listed by Clarivate Analytics/Thomson Reuters Highly Cited Researchers in Engineering in 2014–2020.

Harry L. Trentelman (Life Fellow, IEEE) received the Ph.D. degree in mathematics from the University of Groningen, The Netherlands, in 1985, under the supervision of Jan C. Willems. He is currently a Professor of systems and control with the Bernoulli Institute for Mathematics, Computer Science and Artificial Intelligence, University of Groningen. He is the coauthor of the textbook *Control Theory for Linear Systems* (Springer, 2001). His research interests include behavioral approach to systems and control, robust control, multidimensional linear systems, hybrid systems, analysis, control and model reduction of networked systems, and the geometric theory of linear systems. He was a Senior Editor of the IEEE TRANSACTIONS OF AUTOMATIC CONTROL and an Associate Editor of *Automatica*, *SIAM Journal on Control and Optimization*, and *Systems & Control Letters*.